GEOPHYSICAL RESEARCH LETTERS, VOL. 40, 568–572, doi:10.1029/2012GL054011, 2013

Long range correlations in tree ring chronologies of the USA: Variation within and across species

M. C. Bowers,[1] J. B. Gao,[2,3] and W. W. Tung[1]

Received 25 September 2012; revised 7 December 2012; accepted 10 December 2012; published 14 February 2013.

[1] Tree ring width data are among the best proxies for reconstructing past temperature and precipitation records. The discovery of fractal scaling and long-memory in meteorological and hydrological signals motivates us to investigate such properties in tree ring chronologies. Detrended fluctuation analysis and adaptive fractal analysis are utilized to estimate the Hurst parameter values of 697 tree ring chronologies from the continental United States. We find significant differences in the Hurst parameter values across the 10 species studied in the work. The long-range scaling relations found here suggest that the behavior of tree ring growth observed in a short calibration period may be similar to the general behavior of tree ring growth in a much longer period, and therefore, the limited calibration period may be more useful than originally thought. The variations of the long-range correlations within and across species may be further explored in future to better reconstruct paleoclimatic records. **Citation:** Bowers, M. C., J. B. Gao, and W. W. Tung (2013), Long range correlations in tree ring chronologies of the USA: Variation within and across species, *Geophys. Res. Lett., 40*, 568–572, doi:10.1029/2012GL054011.

1. Introduction

[2] Tree ring width data are abundant and have high temporal resolution. They respond well to environmental conditions such as solar radiation, air temperature, soil temperature, precipitation, soil moisture, and humidity [e.g., *García-Suárez et al*., 2009; *Scharnweber et al*., 2011]. Therefore, they are considered among the best proxies for reconstructing past climate records, and thus have been utilized for a wide variety of applications in paleoclimatology, including reconstruction of past temperature records [e.g., *Mann et al*., 2008; *Zhu et al*., 2008; *Li et al*., 2011]) and past precipitation records [e.g., *Quesne*, 2006; *Griggs et al*., 2007].

[3] It is well known that different species of tree respond differently to certain environmental conditions, e.g., some are more sensitive to temperature variation while others are more sensitive to moisture variation [*García-Suárez et al*., 2009]. To study such sensitivities, one may examine how tree ring annual growth width or density correlates with various environmental factors over a certain calibration period [*Shao et al*., 2010]. Calibration periods are typically much shorter than the periods over which paleoclimate records are reconstructed, which are often on the scale of 10^3 years [e.g., *Mann et al*., 2008; *Loehle*, 2009]. Will problems arise due to limited calibration periods? To gain insights into this issue, we focus on studying scaling and the correlation structure of tree ring time series.

[4] Noticing that temperature, rainfall, and river discharge time series may be reconstructed from tree ring data through simple linear regressions, it may be expected that tree ring data also exhibit the long-range correlations observed in temperature [*Eichner et al*., 2003], rainfall [*Lovejoy and Mandelbrot*, 1985], and streamflow [*Pandey et al*., 1998]. Indeed, long-range correlation has been found in the raw tree ring width time series of two species [*Lavallée and Beltrami*, 2004; *Telesca and Lovallo*, 2010].

[5] This motivates us to systematically examine the long-range correlation properties of tree ring chronologies that cannot be readily captured by low-order auto-regressive modeling. In particular, we will examine how these properties may vary within and across tree species.

[6] The long-range correlation properties of a time series can be conveniently characterized by the Hurst exponent or Hurst parameter H [*Hurst*, 1951]. The Hurst parameter quantifies the persistence of a correlation such that when $0 < H < 1/2$, the signal has anti-persistent correlations; when $H = 1/2$, the signal is memoryless or has short-range correlations; when $1/2 < H < 1$, the signal has persistent long-range correlations; and when $H > 1$ the signal may be non-stationary or have non-trivial trends. The Hurst parameter can be estimated by a variety of methods; however, few of these methods are capable of accurately estimating H when $H > 1$ [*Gao et al*., 2006, 2007]. Therefore, care must be taken when estimating H from tree ring data, because H can often be larger than 1 [*Telesca and Lovallo*, 2010].

[7] One of the few methods capable of accurately estimating H when $H > 1$ is the popular detrended fluctuation analysis (DFA) [*Peng et al*., 1994]. The problem of estimating H when $H > 1$ can also be aptly dealt with by a more recent method called adaptive fractal analysis (AFA) [*Gao et al*., 2011], which performs comparably to DFA in many situations, but may be able to better deal with arbitrary trends in the signal [*Gao et al*., 2011]. Here, these methods are used to characterize the long-range correlation properties of 10 different tree species represented in a database of 697 tree ring chronologies from sites across the continental United States.

2. Data

[8] All of the tree ring site chronologies studied here were obtained from the NOAA Paleoclimatology Program's

[1]Department of Earth, Atmospheric, and Planetary Sciences, Purdue University, West Lafayette, IN, USA.
[2]Department of Mechanical and Materials Engineering, Wright State University, Dayton, OH, USA.
[3]PMB Intelligence LLC, West Lafayette, IN, USA.

Corresponding author: Matthew C. Bowers, Department of Earth, Atmospheric, and Planetary Sciences, Purdue University, 550 Stadium Mall Dr., West Lafayette, IN 47907, USA. (bowers.matt.c@gmail.com)

0094-8276/13/2012GL054011

International Tree Ring Data Bank (ITRDB) at http://www.ncdc.noaa.gov/paleo/treering.html. For consistency, we use only chronologies created from tree ring width samples, excluding those from maximum latewood density. The ITRDB has over 1000 site chronologies from the United States, however, because our purpose is to make statistical comparisons among tree species, we narrow the database to species which have at least 25 site chronologies. This leaves representatives from 10 tree species at 697 sites; locations are mapped in Fig. 1, while the ITRDB tree species codes with their corresponding Latin and common names are listed in Table 1.

[9] Tree ring chronologies are derived as follows. Beginning with multiple core samples from multiple trees at a given site, raw ring width measurements are combined using a process described in *Cook and Holmes* [1986] for convenience, it is summarized in Section 1 of the supplementary material. This procedure is intended to remove the effects of factors other than the controlling environment, such as growth trends in individual trees and intra- and inter-tree variability. This leaves one time series of growth indices per site, intended to serve as a proxy environmental signal capable of reflecting local climatic conditions.

3. Methodology

[10] As pointed out earlier, the Hurst parameter H characterizes the long-range correlations in a time series. There are many effective ways to estimate H [*Gao et al*., 2006, 2007]. Because H for tree ring width data may have $H > 1$ [e.g., *Telesca and Lovallo*, 2010], while most of the methods available, such as fluctuation analysis and rescaled range (R/S) analysis, yield estimates of H that saturate at 1 [*Gao et al*., 2006, 2007], care must be taken to choose the appropriate methods. Here, we choose detrended fluctuation analysis (DFA) [*Peng et al*., 1994], which is the most popular and is not hindered by the saturation problem. We also employ a newer method, adaptive fractal analysis [AFA] [*Gao et al*., 2011], which is comparable to DFA in many situations, but may better deal with arbitrary trends in the signals [*Gao et al*., 2011].

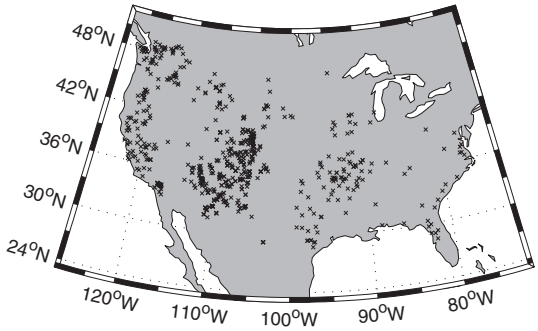

Figure 1. Map showing locations of site chronologies used in the study.

Table 1. Tree Species Information

Species Code	Latin name	Common name
PCGL	*Picea glauca*	Canadian spruce
PIED	*Pinus edulis*	Colorado pinyon
PIFL	*Pinus flexilis*	limber pine
PIPO	*Pinus ponderosa*	ponderosa pine
PSMA	*Pseudotsuga macrocarpa*	bigcone Douglas-fir
PSME	*Pseudotsuga menziesii*	Douglas-fir
QUAL	*Quercus alba*	American white oak
QUDG	*Quercus douglasii*	blue oak
QUST	*Quercus stellata*	American post oak
TADI	*Taxodium distichum*	baldcypress

[11] DFA works as follows: given a noise (or increment) time series, $x_1, x_2, x_3, \cdots$, with mean $\bar{x}$, one first constructs a random walk process,

$$u(i) = \sum_{k=1}^{i} (x_k - \bar{x}), i = 1, 2, \cdots, N \quad (1)$$

[12] One then divides $\{u(i), i = 1, 2, \cdots, N\}$ into $\lfloor N/l \rfloor$ nonoverlapping segments (where $\lfloor N/l \rfloor$ denotes the largest integer equal to or smaller than N/l), each containing l points, and defines the local trend in each segment to be the ordinate of a best linear or polynomial fit of the time series in that segment. Finally, one computes the "detrended walk", denoted by $u_l(n)$, as the difference between the original "walk" $u(n)$ and the local trend. The fractal behavior is described by the following scaling law

$$F_d(l) = \left\langle \sum_{i=1}^{l} u_l(i)^2 \right\rangle^{1/2} \sim l^H \quad (2)$$

[13] where the angle brackets denote ensemble averages of all the segments. The so-called DFA-m denotes the use of an m-order polynomial for the segment fitting. For tree ring data, DFA-1 has been found to be consistent with its higher-order counterparts [*Telesca and Lovallo*, 2010], so in this work, we focus on DFA-1.

[14] AFA first estimates a globally smooth trend signal $v(i)$ for the random walk process $u(i)$, and thus eliminates the problem of abrupt jumps at the boundaries of neighboring segments in DFA.

[15] The residual, $u(i) - v(i)$, characterizes fluctuations around the global trend, and its variance yields the Hurst parameter H according to *Gao et al*. [2011]

$$F(w) = \left[\frac{1}{N} \sum_{i=1}^{N} (u(i) - v(i))^2 \right]^{1/2} \sim w^H. \quad (3)$$

4. Analysis and Results

4.1. Estimation of Hurst Parameter

[16] Based on the log-log plot of $F(w)$ versus w for each tree ring chronology, linear fitting is used to estimate the slope across the power-law scaling region, providing an estimate of H. Examples of this procedure are shown for four site chronologies in Figure 2. The estimates of H are consistent between DFA-1 and AFA, thus the estimates obtained from AFA are used in further analysis.

[17] It is found that for some chronologies studied here, the scaling behavior may only be defined for time scales up to about 33 years, corresponding to the first five points of AFA (see Figure 2d), while for other chronologies, the scaling behavior may be defined for a few hundred years

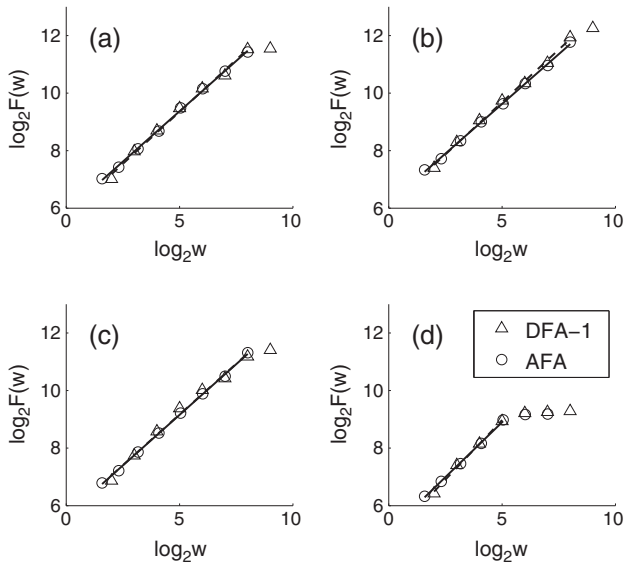

Figure 2. Long-range correlation analysis of tree ring chronologies from (a) Kane Spring, Utah (PIED), (b) Walnut Canyon National Monument, Arizona (PIPO), (c) Spruce Canyon, Colorado (PSME), and (d) Jack's Fork, Missouri (QUST). Circles indicate adaptive fractal analysis (AFA), while triangles indicate detrended fluctuation analysis of order 1 (DFA-1). AFA and DFA-1 are in good agreement for each time series.

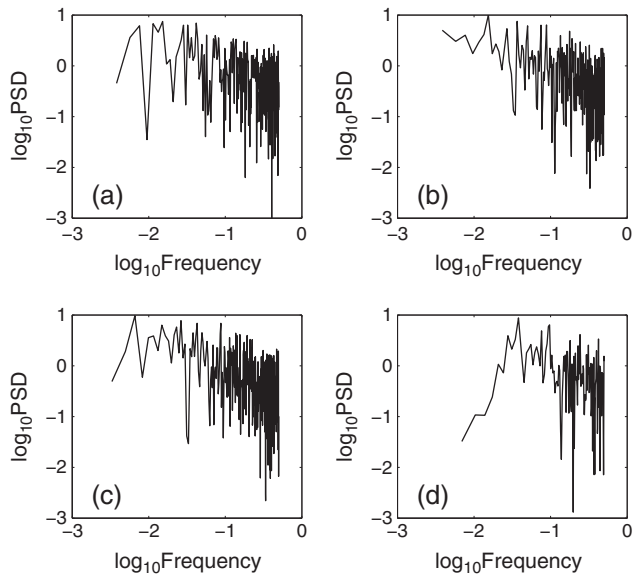

Figure 3. Power spectral density analysis of tree ring chronologies from (a) Kane Spring, Utah (PIED), (b) Walnut Canyon National Monument, Arizona (PIPO), (c) Spruce Canyon, Colorado (PSME), and (d) Jack's Fork, Missouri (QUST).

(see Figures 2a, b, c). For ring data with long scaling regions, the Hurst parameter determined by five points in AFA is similar to that determined by the entire scaling region; thus, in the following analysis, we will only use the first five points in AFA to estimate the Hurst parameter.

[18] Careful examination of the data with shorter scaling ranges reveals that the break in scaling is due to a large cutoff in low frequency variation in the ring data. This is confirmed by the power spectral densities shown in Figure 3.

[19] In particular, note the scaling break in the Jack's Fork chronology in Figure 2d and the corresponding suppression of its low frequency variation in Figure 3d. It is known that the processing of raw tree ring data can lead to loss of low frequency variation in the extracted chronologies [*Cook et al*., 1995; *Briffa and Melvin*, 2011]. This suggests that the limited scaling in some chronologies may not be intrinsic to the data, but due to excessive filtering.

4.2. Variation of Hurst Parameter Within and Across Species

[20] We first checked the variation of H within species. This is best illustrated by estimating the distribution for H for each species using a kernal density estimation method. Four examples are shown in Figure 4. Alternatively, we may use scatter plots as shown in Figure 5.

[21] Based on these results, we can compute sample statistics for the groups, which are given in Table 2. The mean value of H for each species population satisfies $1/2 < H < 1$, indicating long-memory and persistent behavior.

[22] From Table 2 and Figure 5, we also note that there is considerable variation in the mean H value from species to species, suggesting variation in the typical strength of persistence. To quantitatively examine variations of H across species, two procedures are adapted here. One is ANOVA,

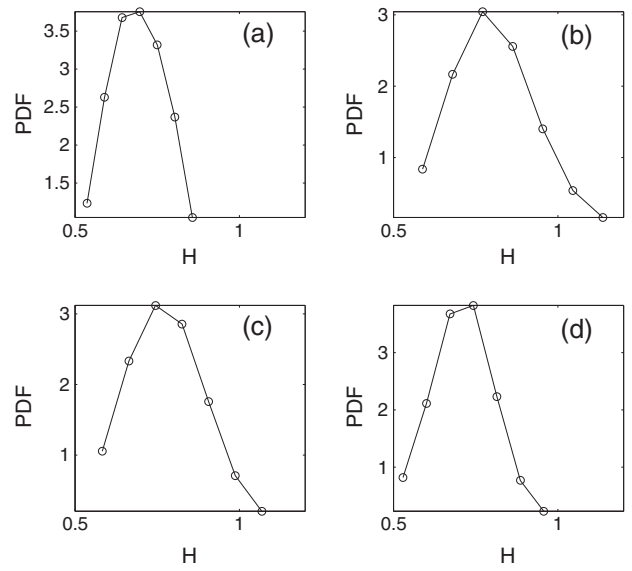

Figure 4. Probability density functions (PDF) of Hurst parameter for tree ring chronologies of (a) Pinyon pine (PIED), (b) Ponderosa pine (PIPO), (c) Douglas fir (PSME), and (d) post oak (QUST). Densities are obtained from kernal PDF estimation.

which tests the hypothesis of equal group means against the alternative of non-equality. The test, which is detailed in Appendix, yields a p-value$\ll$.0001, rejecting the hypothesis of equal group means. This result prompts the use of a multiple comparison procedure, also detailed in the Appendix, to further clarify the variation among species. The results of this analysis, with significance level α=.05, are summarized in Table 2.

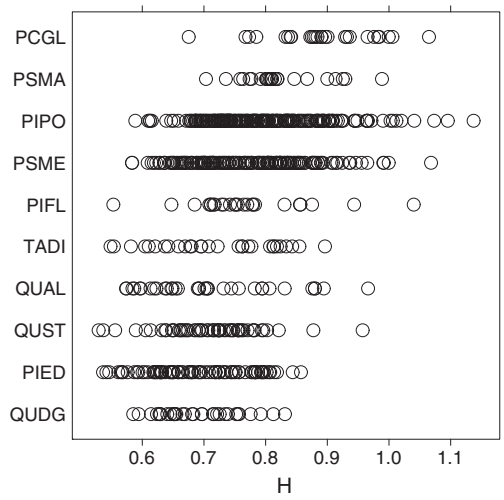

Figure 5. One-dimensional scatter plots of H by species.

Table 2. Summary Statistics of H for Each Species.

Species code	Similar to	Mean	Standard deviation	Sample size
[1]QUDG	2, 3, 4, 5	0.690	0.063	33
[2]PIED	1, 3, 4, 5	0.691	0.079	90
[3]QUST	1, 2, 4, 5, 6	0.709	0.077	57
[4]QUAL	1, 2, 3, 5, 6	0.711	0.105	35
[5]TADI	1, 2,3, 4, 6, 7	0.721	0.096	30
[6]PIFL	3, 4, 5, 7, 8, 9	0.767	0.096	25
[7]PSME	5, 6, 8, 9	0.773	0.093	168
[8]PIPO	6, 7, 9	0.800	0.096	207
[9]PSMA	6, 7, 8, 10	0.823	0.066	25
[10]PCGL	9	0.892	0.085	27

"Similar to" indicates which group means are not significantly different

[23] While it is desirable to find the connections between the long-range correlation properties of tree ring chronologies and climate variability, our exploratory analysis does not find any simple connections, as shown in Section 2 of the supplementary material. Due to potentially large variations in H over short inter-site distances, the most appropriate use of chronology correlation properties may be in spatial aggregations of H to assist with continental-, hemispheric-, or global-scale climate variable reconstructions.

5. Discussions and Conclusions

[24] A database of 697 tree ring chronologies from 10 different tree species across the United States is examined for long-range correlation properties using detrended fluctuation analysis and adaptive fractal analysis. The Hurst parameter H is used to quantify the strength of these correlations. The mean value of H for sites of each species lies in $1/2 < H < 1$, indicating a tendency for persistent behavior. There is variation in the mean H across species within this interval, and analysis of variance and a multiple comparison procedure are used to detect differences in the mean H value among species. The difference in mean Hurst parameter value between certain species is found to be statistically significant.

[25] Our study has two interesting implications. One concerns the usefulness of a limited calibration period, which is often short compared to the time span over which paleoclimatic variables are to be reconstructed. Had tree ring data only exhibited short-range correlations, short calibration periods would indeed have very limited value; fortunately, this is not the case — the self-similarity and long-range correlations in tree ring data implies that the general behavior of tree ring growth would be similar to that observed in the calibration period.

[26] The second implication of our work concerns the reconstruction of paleoclimatic records. One critical question is: how may the tree ring data of different sites of the same species and different species be combined to best reconstruct paleoclimatic records? An intelligent response might be to utilize the value of the Hurst parameters of each site to construct a suitable weighting scheme for sites of the same species, as well as for different species. Development of such a scheme would be an important task in future research.

Appendix A: ANOVA and Multiple Comparison Procedure

[27] ANOVA basically compares two types of variations — within groups and between groups, by assuming [*DeGroot and Schervish*, 2002]:

[28] 1. Observations are independent

[29] 2. Group populations are normally distributed

[30] 3. Group populations have the same variance

[31] To fix the idea, let us consider p groups, where the i-th group having observations $y_{ij}, j = 1, \cdots, n_i$, and mean $\bar{y}_i = \sum_{j=1}^{n_i} y_{ij}/n_i$. Clearly, the global mean is $\bar{y} = \frac{1}{n}\sum_{i=1}^{p} n_i \bar{y}_i$, where $n = \sum_{i=1}^{p} n_i$. The total variation around the global mean may be written as

$$SS_{\text{Total}} = \sum_{i=1}^{p}\sum_{j=1}^{n_i} \left(y_{ij} - \bar{y}\right)^2 = SS_{\text{Within}} + SS_{\text{Between}} \tag{A1}$$

where

$$SS_{\text{Within}} = \sum_{i=1}^{p}\sum_{j=1}^{n_i} \left(y_{ij} - \bar{y}_i\right)^2 \tag{A2}$$

$$SS_{\text{Between}} = \sum_{i=1}^{p} n_i (\bar{y}_i - \bar{y})^2 \tag{A3}$$

[32] The test statistic is obtained from the ratio

$$F = \frac{SS_{\text{Between}}/(p-1)}{SS_{\text{Within}}/(n-p)} \tag{A4}$$

which follows an F-distribution with p-1 and n-p degrees of freedom. When this null hypothesis is not true, the expectation of the ratio will be larger than it would be if the null hypothesis were true. ANOVA gives a criterion for accepting/rejecting the null hypothesis for an observed F under the three basic assumptions. Note that in practice, assumptions (2) and (3) may be weakly violated.

[33] ANOVA is most conveniently carried out in the free software R. In the following examples, '>' indicates a prompt for commands in the R environment. Begin by reading the data from a file `H_species.dat`.

```
> rings <- read.table("H_species.dat",header=TRUE)
```

Table 3. One-way ANOVA test comparing mean values of H among the 10 species.

Source	Sum of squares	df	Mean squares	F	Prob > F
Groups	1.7880	9	0.1987	24.6836	≪.0001
Error	5.5294	687	0.0080		
Total	7.3174	696			

"Groups" indicates variation between groups, while "Error" indicates variation within groups.

[34] Now the dataframe `rings` has two columns: H (observations) and species (groups). We can execute the ANOVA test and view the results.

```
> aov.rings <− aov(H~species,data=rings)
> summary(aov.rings)
```

[35] The results of this one-way ANOVA test for differences in group mean H are given in Table 3. The small p-value indicates that the hypothesis of equal group means is rejected at any reasonable significance level.

[36] Now that ANOVA has indicated differences among the groups, we need to determine whether two tree chronologies have the same mean Hurst parameter or not. Intuitively, when the difference between the means of two groups of observations is large compared with the summation of the two standard deviations, the groups may be considered to have different means. When there are only two groups, taking into account the effect of sample size, this idea leads to the t-test. When there are more than two groups, a procedure, called Tukey HSD (honestly significant difference) multiple comparison, can fix the probability α of falsely identifying differences in group means, for the entire set of pairwise comparisons, rather than for each pair individually. This reduces the overall chance of incorrectly rejecting the null hypotheses, and therefore, Tukey HSD multiple comparison is more suitable than a simple sequence of pairwise t-tests.

[37] We can carry out the Tukey HSD procedure with α=.05 in R as follows.

```
> tuk <− TukeyHSD(aov.rings)
> print(tuk)
```

[38] The resulting R output gives a 95% confidence interval around the difference between each pair of group means. If the interval does not contain 0, then the true difference in group means is likely non-zero, and we consider the difference significant. For example, the first row of the output table is:

```
                diff          lwr        upr     p adj
PIED-QUDG 0.001274444 -0.056677522 0.05922641 1.0000000
```

[39] where `diff` is the difference between group means of PIED and QUDG, `lwr` and `upr` are respectively the lower and upper confidence limits for the difference in group means, and `p adj` is the p-value after adjustment for the multiple comparisons. Here we see that the confidence interval about the difference in means between groups PIED and QUDG contains 0. Thus, there is not a significant difference in the two group means.

[40] **Acknowledgments.** The authors thank Professor Bo Li for useful discussions. The work is supported in part by NSF grants CMMI-1031958 and 0826119.

References

Briffa, K. R., and T. M. Melvin (2011), A closer look at regional curve standardization of tree-ring records: Justification of the need, a warning of some pitfalls, and suggested improvements in its application, in *Dendroclimatology, Developments in Paleoenvironmental Research*, vol. *11*, edited by M. K. Hughes, T. W. Swetnam, and H. F. Diaz, pp. 113–145, Springer Netherlands.

Cook, E., and R. L. Holmes (1986), Users Manual for Program ARSTAN, in *Tree-Ring Chronologies of Western North America: California, eastern Oregon and northern Great Basin*, edited by R. L. Holmes, R. K. Adams and H. C. Fritts, pp. 50–65, Laboratory of Tree-Ring Research, The University of Arizona.

Cook, E. R., et al. (1995), The "segment length curse" in long tree-ring chronology development for paleoclimatic studies, *Holocene*, *5*, 229–237.

DeGroot, M. H., and M. J. Schervish (2002), *Probability and Statistics*, 3rd ed., Addison-Wesley.

Eichner, J. F., E. Koscielny-Bunde, S. Havlin, and H. J. Schellnhuber (2003), Power-law persistence and trends in the atmosphere: a detailed study of long temperature records, *Phys. Rev. E*, *68*, 046133.

Gao, J., et al. (2006), Assessment of long-range correlation in time series: How to avoid pitfalls, *Phys. Rev. E*, *73*(016117).

Gao, J., J. Hu, and W. Tung (2011), Facilitating joint chaos and fractal analysis of biosignals through nonlinear adaptive filtering, *PLoS One*, *6*(9), e24,331.

Gao, J. B., Y. H. Cao, W. W. Tung, and J. Hu (2007), *Multiscale Analysis of Complex Time Series — Integration of Chaos and Random Fractal Theory, and Beyond*, Wiley.

García-Suárez, A., C. Butler, and M. Baillie (2009), Climate signal in tree-ring chronologies in a temperate climate: A multi-species approach, *Dendrochronologia*, *27*, 183–198.

Griggs, C. B., A. T. DeGaetano, P. I. Kuniholm, and M. W. Newton (2007), A regional high-frequency reconstruction of May-June precipitation in the north Aegean from oak tree-rings, A.D. 1089–1989, *Int. J. Climatol.*, *27*(8), 1075–1089.

Hurst, H. E. (1951), Long-term storage capacity of reservoirs, *Trans. Am. Soc. Civ. Eng.*, *116*, 770–808.

Lavallée, D., and H. Beltrami (2004), Stochastic modeling of climatic variability in dendrochronology, *Geophys. Res. Lett.*, *31*(L15202).

Li, Z. S., Q. B. Zhang, and K. Ma (2011), Tree-ring reconstruction of summer temperature for A.D. 1475–2003 in the central Hengduan Mountains, Northwestern Yunnan, China, *Clim. Chang.*, *110*, 455–467.

Loehle, C. (2009), A mathematical analysis of the divergence problem in dendroclimatology, *Clim. Chang.*, *94*, 233–245.

Lovejoy, S., and B. Mandelbrot (1985), Fractal properties of rain and a fractal model, *Tellus*, *37A*, 209–232.

Mann, M. E., et al. (2008), Proxy-based reconstructions of hemispheric and global surface temperature variations over the past two millennia, *Proc. Natl. Acad. Sci.*, *105*(36), 13,252–13,257.

Pandey, G., S. Lovejoy, and D. Schertzer (1998), Multifractal analysis of daily river flows including extremes for basins of five to two million square kilometers, one day to 75 years, *J. Hydrol.*, *208*, 62–81.

Peng, C., et al. (1994), Mosaic organization of DNA nucleotides, *Phys. Rev. E*, *49*, 1685–1689.

Quesne, C. L. (2006), Ancient *Austrocedrus* tree-ring chronologies used to reconstruct central Chile precipitation variability from A.D. 1200 to 2000, *J. Climate*, *19*, 5731–5744.

Scharnweber, T., et al. (2011), Drought matters—Declining precipitation influences growth of *Fagus sylvatica L.* and *Quercus robur L.* in north-eastern Germany, *For. Ecol. Manage.*, *262*, 947–961.

Shao, X., et al. (2010), Climatic implications of a 3585-year tree-ring width chronology from the northeastern Qinghai-Tibetan Plateau, *Quaternary Sci. Rev.*, *29*, 2111–2122.

Telesca, L., and M. Lovallo (2010), Long-range dependence in tree-ring width time series of *Austrocedrus chilensis* revealed by means of the detrended fluctuation analysis, *Physica A*, *389*, 4096–4104.

Zhu, H., et al. (2008), Millennial temperature reconstruction based on tree-ring widths of Qilian juniper from Wulan, Qinghai Province, China, *Chinese Sci. Bull.*, *53*(24), 3914–3920.